1 **Anthropogenic amplification of biogenic secondary organic aerosol production**
2

4 Yiqi Zheng[1,2,*], Larry W. Horowitz[3], Raymond Menzel[3], David J Paynter[3], Vaishali Naik[3], Jingyi
5 Li[4], Jingqiu Mao[1,2,*]
6
7
8 [1]Geophysical Institute, University of Alaska Fairbanks, Fairbanks, AK, USA
9 [2]Department of Chemistry and Biochemistry, University of Alaska Fairbanks, AK, USA
10 [3]NOAA Geophysical Fluid Dynamics Laboratory, Princeton, NJ, USA
11 [4]School of Environmental Science and Engineering, Nanjing University of Information Science
12 and Technology, Nanjing, China
13
14
15 *Correspondence to Yiqi Zheng (zhengyiqi1989@gmail.com) and Jingqiu Mao
16 (jmao2@alaska.edu)

18

1 **Abstract**
2
3 Biogenic secondary organic aerosols (SOA) contribute to a large fraction of fine aerosols globally,
4 impacting air quality and climate. The formation of biogenic SOA depends on not only emissions
5 of biogenic volatile organic compounds (BVOCs) but also anthropogenic pollutants including
6 primary organic aerosol, sulfur dioxide (SO_2), and nitrogen oxides (NO_x). However, the
7 anthropogenic impact on biogenic SOA production (AIBS) remains unclear. Here we use the
8 decadal trend and variability of observed OA in the southeast US, combined with a global
9 chemistry-climate model, to better constrain AIBS. We show that the reduction in SO_2 emissions
10 can only explain 40% of the decreasing decadal trend of OA in this region, constrained by the low
11 summertime month-to-month variability of surface OA. We hypothesize that the rest of OA
12 decreasing trend is largely due to reduction in NO_x emissions. By implementing a scheme for
13 monoterpene SOA with enhanced sensitivity to NO_x, our model can reproduce the decadal trend
14 and variability of OA in this region. Extending to centennial scale, our model shows that global
15 SOA production increases by 36% despite BVOC reductions from preindustrial period to present
16 day, largely amplified by AIBS. Our work suggests a strong coupling between anthropogenic and
17 biogenic emissions in biogenic SOA production that is missing from current climate models.
18
19

1 **1. Introduction**
2 Terrestrial vegetation emits more than 1 Pg per year of BVOCs(Guenther et al., 2012), leading to
3 a major source of SOA in the atmosphere(Goldstein and Galbally, 2007). SOA exerts significant
4 impacts on climate, air quality and human welfare(Shrivastava et al., 2017; Pye et al., 2021), but
5 is not well represented in climate models. Global climate models differ largely in simulated SOA
6 burden, variability, and radiative effects(Tsigaridis et al., 2014) due to complexity associated with
7 emission of precursors, multiphase chemical and physical processes, aging, radiative properties,
8 and other processes(Shrivastava et al., 2017). Many climate models simply scale SOA yield with
9 BVOC precursors(Horowitz et al., 2020; Carslaw et al., 2013; Koch et al., 2011).
10
11 Current understanding of biogenic SOA formation has advanced far beyond this simple scaling of
12 BVOC emissions. SOA formation from BVOC oxidation is largely dependent on its oxidants
13 (OH/O_3/NO_3) and the yields show non-linear behavior under different NO_x conditions(Ng et al.,
14 2017; Presto et al., 2005). One advanced scheme is the Volatility Basis Set (VBS), in which
15 intermediate semivolatile products from the oxidation of BVOCs are grouped into volatility bins
16 and can reversibly condense onto pre-existing organic aerosols(Donahue et al., 2006; Pye et al.,
17 2010). VBS accounts for the dependence of SOA formation on atmospheric oxidants, NO_x-
18 dependent chemical regimes, POA and temperature. Some studies showed that VBS schemes
19 underestimated observations and that photochemical aging schemes with varying complexity may
20 improve simulation results in different regions and seasons(Zheng et al., 2015; Robinson et al.,
21 2007; Oak et al., 2022). Another pathway is through reactive uptake of smaller molecules onto
22 aqueous aerosols. Several isoprene oxidation products, such as epoxides (IEPOX)(Paulot et al.,
23 2009) and glyoxal(Liggio, 2005; Li et al., 2016), though often not directly condensable due to their
24 high equilibrium vapor pressure, can undergo aqueous phase reactions and oligomerize in the
25 condensed phase. The detailed mechanism is complicated by aerosol acidity, composition, and
26 coating(Shrivastava et al., 2017). These advancements highlight the role of anthropogenic
27 emissions modulating biogenic SOA formation through nitrogen oxides (NO_x), SO_2 and primary
28 organic aerosol (POA).
29
30 One major uncertainty is to what extent anthropogenic emissions modulate biogenic SOA
31 formation. In the southeast US (SEUS), a region largely covered by natural vegetation and also
32 heavily populated, organic aerosol shows a decreasing trend in the recent two decades(Kim et al.,
33 2015; Attwood et al., 2014), likely due to reductions in POA (Blanchard et al., 2016; Ridley et al.,
34 2018), sulfate and aerosol water (Christiansen et al., 2020; Ridley et al., 2018; Marais et al., 2017;
35 Malm et al., 2017; Blanchard et al., 2016) and NO_x (Zheng et al., 2015; Xu et al., 2015; Pye et al.,
36 2019). Several studies suggest that SO_2 largely modulates SOA through reactive uptake of
37 IEPOX(Pye et al., 2013; Marais et al., 2017), but the acidity-catalyzed sulfate uptake mechanism
38 appears to overestimate the trend of OA reduction in the SEUS(Zheng et al., 2020). The role of
39 NO_x remains unclear. While SOA yield generally decreases with NO_x level due to fragmentation
40 of large molecules (Kroll and Seinfeld, 2008), recent studies show that NO_x can in fact increase
41 SOA production (Zheng et al., 2015; Xu et al., 2015; Pye et al., 2019; Pullinen et al., 2020). The
42 combined effect of NO_x, SO_2 and POA can be significant (Carlton et al., 2010; Hoyle et al., 2011),
43 but remain unconstrained by ambient observations.
44
45 Here we use the decadal trend and variability of observed OA in the southeast US, combined with
46 other observational datasets and a global chemistry-climate model (GFDL AM4.1)(Horowitz et

al., 2020), to better constrain the anthropogenic impact on biogenic SOA production (AIBS). We use three schemes (summarized in Table 1 and detailed in Methods), Simple, CMPX, and CMPX_ag, to investigate the AIBS from decadal to centennial time scales.

2. Methods

2.1 GFDL AM4.1

The Geophysical Fluid Dynamics Laboratory (GFDL)'s Atmospheric Model version 4.1 (AM4.1)(Horowitz et al., 2020) is a three-dimensional global chemistry-climate model that includes interactive simulation of stratospheric chemistry and tropospheric O_3-NO_x-CO-VOC and bulk aerosol chemistry, allowing explicit treatment of aerosol reactive uptake of IEPOX and glyoxal(Li et al., 2016, 2018; Mao et al., 2013). Community Emissions Data System (CEDS) are used for historical anthropogenic emissions from 1849 to 2016. Global fire emissions are based on Global Fire Emissions Database version 4 (GFED4), the Fire Modeling Intercomparison Project (FireMIP), visibility-observations and Global Charcoal Database (GCD). Biogenic isoprene and monoterpene emissions are calculated online by the Model of Emissions of Gases and Aerosols from Nature version 2.1 (MEGAN2.1), using empirical functions of plant-functional-type (PFT)-specific emission basal factors, leaf area index (LAI), temperature and light. LAI and PFTs are prescribed at the 1992 level. Dependence of soil moisture, O_3 and CO_2 are neglected due to large uncertainties. Radiative effects of SOA is calculated assuming SOA is externally mixed from other aerosols(Horowitz et al., 2020), although ISOA is formed through sulfate uptake in the chemistry module.

We perform simulations for years 1998-2016 for present day (PD) and 1870-1888 for pre-industrial period (PI). In each simulation, the first two years are discarded as spin-up. The remaining 17 years are used for analysis. The PD simulations are nudged with reanalysis winds from NCEP-DOE Reanalysis 2. The PI simulations are free running with no nudging. All simulations are driven by observed or reconstructed sea surface temperature and sea-ice(Horowitz et al., 2020). In the two PI simulations, we scale up the isoprene and monoterpene emission basal factors by 35% to account for the higher natural vegetation cover at pre-industrial period than today, equivalent to a 26% reduction of natural vegetation cover from PI to PD(Unger, 2014). We apply this single scaling factor to BVOC emission basal factors as an idealized study instead of using reconstructed land cover type and LAI to avoid uncertainties in historical vegetation reconstructions.

2.2 Modeling of SOA formation

In GFDL AM4.1, SOA is composed of anthropogenic SOA (ASOA), isoprene SOA (ISOA) and monoterpene SOA (TSOA). ASOA is formed through the oxidation of C_4H_{10} by OH in all simulations. In the default "Simple" scheme, ISOA and TSOA are assumed to be produced with a pseudo-emission equivalent to a 10% per-carbon yield of the interactively calculated isoprene and monoterpene emissions, respectively.

In the updated "CMPX" scheme, isoprene and monoterpenes are oxidized by OH, O_3 and NO_3. TSOA is calculated by a 4-product Volatility Basis Set (VBS) summarized in Table 1. Organic peroxy radicals (RO_2) formed from OH- and O_3-initiated oxidation of monoterpene can react with NO under high-NO_x conditions and with HO_2 under low-NO_x conditions. The low-NO_x pathway (RO_2+HO_2) has higher yields for SOA than the high-NO_x pathway (RO_2+NO)(Pye et

1 al., 2010; Zheng et al., 2015). The branching ratio between the low- versus high-NO_x pathways
2 are defined as:
3
4
$$\beta_{NO} = \frac{k_{RO2+NO} * [NO]}{k_{RO2+NO} * [NO] + k_{RO2+HO2} * [HO_2]}$$
5
6 Where k_{RO2+NO} and $k_{RO2+HO2}$ represent the reaction rate coefficients of RO_2+NO and RO_2+HO_2,
7 respectively. At nighttime, the NO_3-initiated oxidation of monoterpenes has a high yield of
8 organic nitrates and contributes a significant amount of SOA(Ng et al., 2017).

9 In an additional configuration, we further implement a simplified photochemical aging
10 parameterization to the semivolatile oxidation products of terpenes in the CMPX scheme
11 (CMPX_ag)(Zheng et al., 2015), to account for the decrease in volatility as a result of OH
12 oxidation(Donahue et al., 2012). We apply a rate constant of $k_{OH} = 4\times10^{-11}$ cm^3 $molec^{-1}$ s^{-1}
13 (Robinson et al., 2007), in line with recent estimates of 2-4 $\times10^{-11}$ cm^3 $molec^{-1}$ s^{-1} for terpene
14 SOA(Donahue et al., 2012; Isaacman-VanWertz et al., 2018). As we show below, the aging
15 increases the SOA burden as well as the sensitivity of SOA to NO_x, improving the model
16 underestimate of SOA by the VBS scheme.
17
18 ISOA is computed through the aqueous-phase uptake of IEPOX and glyoxal onto sulfate aerosol.
19 The uptake coefficients for IEPOX and glyoxal are set to 0.001, different than previous studies
20 using higher or acidity-dependent uptake coefficients(Marais et al., 2016; Lin et al., 2014a). This
21 is supported by the OA month-to-month variability (MMV) in summer and its decadal trend over
22 the southeast US, as a previous model with acidity-dependent uptake coefficients shows too high
23 of MMV and too much OA in the early 2000s(Zheng et al., 2020). The uptake rate coefficients
24 can be even lower due to the effect of aerosol-phase state (Zhang et al., 2018b). To avoid
25 uncertainties associated with aerosol acidity, relative humidity, and coating effect, we here apply
26 uptake coefficient of 0.001 for both IEPOX and glyoxal. This leads to good agreement between
27 our model and observation in the SEUS on both OA magnitude and summertime MMV (Figure1,
28 S1, S2 and S13). The details of the Simple, CMPX, and CMPX_ag schemes are summarized in
29 Table 1.
30
31 **2.3 Observational datasets**
32 For model evaluation we use filter measurement of organic carbon from two surface aerosol
33 measurement networks in the US: IMPROVE (the Interagency Monitoring of Protected Visual
34 Environments)(Solomon et al., 2014) and SEARCH (the SouthEastern Aerosol Research and
35 Characterization)(Edgerton et al., 2005). We focus on the southeast US which is both heavily
36 vegetated and populated. We select 20 IMPROVE sites and 3 SEARCH rural sites within the
37 southeast US region (29-37°N, 74-96°W). We apply a seasonal-dependent ratio to convert organic
38 carbon to organic aerosol (OA) mass: 2.2 in June-July-August, 1.8 in December-January-February
39 and 1.9 in other months(Philip et al., 2014).
40
41 We also compare modeling results to OA measurement by Aerosol Chemical Speciation Monitor
42 (ACSM). We select 3 European sites from the ACTRIS (the Aerosol, Clouds and Trace Gases
43 Research Infrastructure) network: Hyytiala (Finland), Puy de Dome (France) and Birkenes II
44 (Norway); two sites from the ARM (Atmospheric Radiation Measurement) network: Southern

1 Great Plains (US) and Manacapuru, Amazonia (Brazil). These sites are covered by natural
2 vegetation and have more than a year's worth of data available.
3
4
5 **3. Results**
6 **3.1 Decadal trend of summertime OA in SEUS and its variability**
7 The SEUS is a region heavily influenced by both biogenic and anthropogenic emissions(Mao et
8 al., 2018). In the last two decades, organic aerosol shows a decreasing trend, resulting from
9 reductions in anthropogenic pollutants including SO_2 and NO_x (Marais et al., 2017; Blanchard et
10 al., 2016; Ridley et al., 2018). Both CMPX_ag and CMPX schemes can reproduce the summertime
11 surface OA concentrations measured from SEARCH and IMPROVE networks(Solomon et al.,
12 2014; Edgerton et al., 2005), at 4-5 $\mu g/m^3$ as shown in Figure 1, while the Simple scheme has a
13 slight overestimate ($\sim$ 7 $\mu g/m^3$).
14
15 We first examine the simulated decadal OA trend in the SEUS against filter-based measurements
16 from IMPROVE and SEARCH networks (Methods). From 2000 to 2016, the measured summer
17 OA declines by -0.13 $\mu g/m^3$/year from SEARCH and by -0.09 $\mu g/m^3$/year from IMPROVE, both
18 at a reduction rate of -2.3%/year (Figure 1a). This decreasing trend is well reproduced by the
19 CMPX_ag simulation with a decrease of -0.11 $\mu g/m^3$ (-2.0%) per year (Figure 1a), less so with the
20 CMPX scheme (-1.4%/year). In contrast, the Simple scheme shows a slight increase (+0.7%/year)
21 in surface OA due to lack of AIBS and little change of POA in 2000-2016 in this region (Figure
22 1c).
23
24 We further examine the summertime month-to-month variability of surface OA. We find that both
25 CMPX_ag and CMPX schemes can well reproduce the low summertime month-to-month
26 variability of surface OA (standard deviation smaller than 2 $\mu g/m^3$) constrained by IMPROVE and
27 SEARCH measurements (Figure S5), using fixed uptake coefficients (γ=0.001) of IEPOX and
28 glyoxal. This summertime month-to-month variability was found to be too high (standard
29 deviation up to 5 $\mu g/m^3$) in the early 2000s using an acidity-dependent IEPOX reactive uptake
30 scheme(Marais et al., 2016, 2017), pointing to additional species besides SO_2 driving the
31 decreasing OA trend.
32
33 One unique feature of the CMPX_ag simulation is the dominance of TSOA (Figure 1), mainly
34 through enhanced sensitivity of TSOA production to NO_x. Such dominance of TSOA in this region
35 is also supported by recent field observations(Xu et al., 2018; Zhang et al., 2018a). We find TSOA
36 contributes to 60% of the surface OA trend in the CMPX_ag scheme, mainly through NO_x
37 reduction. The NO_3-initiated pathway contributes to the majority of surface TSOA decrease
38 (Figure S3), resulting from the rapid decrease of NO_3 (Figure 1d)(Boyd et al., 2017; Rollins et al.,
39 2012). Compared to the CMPX scheme, the dominant contribution of TSOA is largely due to the
40 OH aging effect, which amplifies the SOA yield from all monoterpene oxidation channels. As a
41 result, we find that NO_x reduction accounts for 60% of OA decrease in SE US. This enhanced
42 sensitivity to NO_x, resonates with recent developments on monoterpene-derived highly
43 oxygenated organic molecules or autooxidation(Pye et al., 2019), highlighting the importance of
44 NO_x in AIBS.
45

1   ISOA contributes to 40% of surface OA trend in the CMPX_ag scheme, mainly through SO_2
2   reduction. The decrease in surface ISOA, at -0.05 μg/m^3/year, is associated with the strong
3   reduction in sulfate (-7%/year). The rapidly decreasing sulfate, NO_x and O_3 in the model are
4   consistent with observations over the SEUS (Figure S4) and previous studies(Zheng et al., 2020;
5   Wells et al., 2021; Simon et al., 2015). In contrast to Marais et al. (2017), we find that this
6   nondominant role of ISOA brings model into much better agreement with observations, especially
7   on the low summertime month-to-month variability of surface OA (standard deviation smaller than
8   2 μg/m^3) constrained by IMPROVE and SEARCH measurements (Figure S5)(Zheng et al., 2020).
9   The observed summertime month-to-month variability also implies a weaker dependence of OA
10   to sulfate aerosols in this region than as shown in Marais et al. (2017), highlighting the importance
11   of TSOA.
12
13   We find a similar trend of summer OA column concentration to the surface OA trend in the model.
14   The CMPX_ag simulation suggests a decreasing trend in summer OA column concentration,
15   driven by both TSOA (-0.13 mg/m^2/year) and ISOA (-0.12 mg/m^2/year) (Figure 1b). Similar to
16   the surface, the aging effect increases the column production of TSOA in CMPX_ag and its
17   sensitivity to changes in NO_x compared with the CMPX scheme.
18
19   **3.2 Present-day OA in vegetated regions and global budget**
20   We further evaluate the modeled OA against measurements by Aerosol Chemical Speciation
21   Monitor (ACSM) in other vegetated regions (Figure S6). In 3 European sites from the ACTRIS
22   network (Methods)(Crenn et al., 2015), all model simulations underestimate measured OA. One
23   possible reason is uncertainties associated with BVOC emissions and biogenic SOA. Jiang et al.
24   (Jiang et al., 2019) showed that MEGAN overestimates isoprene emission but underestimates
25   monoterpene emissions in Europe by a factor of 3. At the Amazon and US sites from the ARM
26   network(Uin et al., 2019), the CMPX_ag scheme successfully captures the measured OA
27   magnitude and seasonal variation. The Simple scheme overestimates the surface OA in Amazon.
28   In the SEUS compared to filter measurements, all simulations show lower OA in winter than
29   observations (Figure S6), likely due to an underestimate of wintertime emissions of
30   POA(Tsigaridis et al., 2014; Liu et al., 2021). In general, the updated CMPX_ag and CMPX
31   schemes agree well with observations in the Amazon and US where biogenic emissions are high.
32
33   Globally, the SOA burden from the Simple, CMPX and CMPX_ag schemes are 0.99, 0.50 and
34   1.05 Tg, respectively, and their SOA production rates are 82, 40 and 69 Tg/year (Figure 2), in
35   agreement with other global modeling studies. The AeroCom phase II model intercomparison
36   summarizes a median SOA source of 51 Tg/year with a range between 16 to 121
37   Tg/year(Tsigaridis et al., 2014), although top-down methods indicate SOA source could be up to
38   50-380 Tg/year(Spracklen et al., 2011). Uncertainties associated with BVOC emissions contribute
39   to the wide spread of SOA estimate by global models. In GFDL AM4.1, annual isoprene and
40   monoterpene emissions are computed to be 505±14 and 137±5 Tg/year, respectively (Figure 2), in
41   line with previous estimates(Guenther et al., 2012).
42
43   Detailed SOA budgets for the three schemes are summarized in Table 2. The CMPX and
44   CMPX_ag schemes have much less ISOA than the Simple scheme as the latter has high pseudo
45   emission of isoprene SOA, which is 10% in GFDL AM4.1 as compared to 3% used in other global
46   models like GEOS-Chem(Pai et al., 2020; Henze and Seinfeld, 2006). ISOA (22.2 Tg/year) and

1   TSOA (14.4 Tg/year) in the CMPX scheme are consistent with previous estimate by GEOS-
2   Chem(Pai et al., 2020; Zheng et al., 2020). The CMPX_ag scheme has higher TSOA (44 Tg/year)
3   than CMPX and Simple due to the aging effect of semivolatile oxidation products from terpenes
4   (Figure 2), and is close to the high end of estimate (12.7-40 Tg/year) by AeroComII(Tsigaridis et
5   al., 2014). ASOA is often neglected by global models despite an estimate of 13.5 Tg/year
6   suggesting ASOA as a non-negligible source(Tsigaridis et al., 2014). In GFDL AM4.1, ASOA
7   (3.3 Tg/year) only considers oxidation of C_4H_{10}, which does not well represent all ASOA and
8   warrants further research.

10   **3.3 Centennial change in biogenic SOA and direct radiative forcing**
11   We now extend our analysis of AIBS from the decadal scale to the centennial scale. To represent
12   the higher natural vegetation cover during PI, we scale up isoprene and monoterpene emission
13   basal factor in the PI simulations by 35%, equivalent to a 26% reduction of natural vegetation
14   cover from PI to PD(Unger, 2014). This simple scaling should be considered as an idealized study
15   to avoid uncertainties associated with historical vegetation reconstruction and the complex role of
16   CO_2 including both fertilization and inhibition effects. From 1870s to 2000s, the simulated
17   isoprene emissions decrease from 632±15 to 505±14 Tg/year (-20%) and monoterpene emissions
18   decrease from 161±5 to 137±5 Tg/year (-15%) (Figure 2), consistent with previous studies(Heald
19   and Spracklen, 2015).

21   Despite the reduction in BVOC emissions from PI to PD, we show a significant increase of
22   biogenic SOA (Figure 2), resulting from increase in anthropogenic emissions and amplified by
23   AIBS. With an increase by 1.4, 7, and 4 for emissions of POA, SO_2 and NO_x, total SOA production
24   increases by 36% and its burden increases by 42% (in the CMPX_ag scheme). ASOA, ISOA and
25   TSOA contribute 17%, 62%, and 21% to the changes in total SOA production, respectively. In
26   contrast, the Simple scheme shows a decrease of SOA production following the reduction in
27   BVOC emissions (Figure 2b). The large increase of SOA from PI to PD differs from previous
28   estimates(Spracklen et al., 2011; Heald and Spracklen, 2015; Zhu et al., 2019; Scott et al., 2017;
29   Lin et al., 2014b; Heald and Geddes, 2016; Hoyle et al., 2009), largely due to AIBS constrained
30   by observations.
31

32   The total PI-to-PD SOA rise is largely dominated by ISOA (62%), resulting from the strong
33   increase in anthropogenic SO_2 emissions and uptake of IEPOX and glyoxal onto sulfate aerosols.
34   The global burden of sulfate aerosol has doubled from 0.7 Tg at PI to 1.6 Tg at PD, with large
35   increase over the tropics, SEUS, and Eurasia (Figure S11). The increase in TSOA is due to both
36   increased NO_x emissions and POA emissions. In contrast to the decadal trend where β_{NO} barely
37   changes, the PI-to-PD increase of TSOA due to the change of NO_x is suppressed by the shift of
38   β_{NO}. The branching ratio β_{NO} increases from a global average of 0.32 at PI to 0.61 at PD (Figure
39   S12), indicating a shift from low-NO_x pathway (higher yields) to high-NO_x pathway (lower yields)
40   for the OH- and O_3-initiated oxidation. These competing effects lead to a net +10% change in
41   TSOA production and a +14% increase in burden from PI to PD. The PI-to-PD change in TSOA
42   in the CMPX scheme is small (-7% in production and +6% in burden). Increased POA provides
43   more organic mass for monoterpene oxidation products to condense on, especially in central Africa
44   and central South America (Figure S11).
45

The large increase of biogenic SOA leads to a cooling direct radiative forcing (DRF) from PI to PD, opposed to the warming suggested by the Simple scheme. DRF is usually defined as the difference between PI and PD direct radiative fluxes at top-of-atmosphere (TOA) under all-sky conditions. We show in Figure 3 the global instantaneous DRF at top-of-atmosphere (TOA) of -(26–44) mW/m^2, comparable to that of POA(-98 mW/m^2). In contrast, the Simple scheme shows a warming DRF of +17 mW/m^2, largely due to lack of AIBS. The DRF of SOA in the updated schemes resides within reported AeroComII estimates, which ranges from -210 to -10 mW/m^2, with a mean value of -60 mW/m^2 and a median value of -20 mW/m^2(Myhre et al., 2013). Due to this increase of SOA burden, our results may also imply a large indirect radiative forcing from biogenic SOA that is missing from previous work(Carslaw et al., 2013).

4. Summary

Our work suggests a strong coupling between anthropogenic and biogenic emissions in biogenic SOA production. Constrained by observations in SEUS, we show that the summertime OA decreasing trend is likely driven by reduction in both NO_x and SO_2 emissions, through TSOA and ISOA. SO_2 alone cannot explain this trend. Our results also point to the importance role of NO_x on modulating biogenic SOA, in line with recent understanding on autooxidation(Pye et al., 2019), although further studies are warranted. The success of the updated schemes in capturing the observed OA trend and month-to-month variability provides confidence in model simulations over longer time scales. At centennial scale, ISOA dominates the total SOA change as a result of a significant rise in global sulfate aerosol from PI to PD, especially in the fast-developing regions like Africa, Middle East, India, and China. POA increases greatly in central Africa and central South America as well as India and east China, which enhances TSOA production. The significant increase in SOA due to AIBS in these regions poses new challenges to meet the World Health Organization's recommendation on annual fine particulate matter exposure (5 μg/m^3)(Pai et al., 2022). Under future scenarios with reduced emissions of SO_2, NO_x and POA, the AIBS may indicate larger reductions in SOA than current model predictions.

The updated SOA scheme in GFDL AM4.1 shows an advance in representing vegetation-chemistry-climate interactions than the default model which assumes fixed yields of SOA from biogenic hydrocarbons, although a variety of uncertainties still exist in the evaluation of SOA and its climate impact. First, the model likely underestimates wintertime POA in the US, total OA in Europe and anthropogenic SOA globally, and the model does not consider absorbing SOA or brown carbon which could form from biomass burning and aging(Tsigaridis and Kanakidou, 2018). The model applies the same optical parameters for all SOA as hydrophilic POA. Second, we use a simplified aging parameter to represent the enhanced SOA sensitivity of NO_x. This should be improved by more explicit schemes on autooxidation (Pye et al., 2019) and organic nitrates(Takeuchi and Ng, 2019). Properties that influence the multiphase growth of SOA, including coating and viscosity, are also not implemented in our model(Shrivastava et al., 2017). The model does not consider nucleation of extremely low volatile compounds from BVOC oxidation, which may increase SOA in pristine environments in the pre-industrial period, thus reducing the PI-to-PD radiative forcing of SOA(Gordon et al., 2016; Zhu et al., 2019). These uncertainties warrant further research in studies on anthropogenic-influenced SOA in climate models.

Acknowledgements

We acknowledge funding from NOAA grant NA18OAR4310114 and NASA grant 80NSSC21K0428. We thank Fabien Paulot and Songmiao Fan for internal GFDL review and support from GFDL's Model Development Team, Modeling Systems Division, Operations group, and the RDHPCS supercomputing resources. We also acknowledge the Electric Power Research Institute (EPRI) and Southern Company for support of the SEARCH network and Atmospheric Research & Analysis, Inc; the US Environmental Protection Agency (EPA) for support of the IMPROVE network and Air Quality System; the European Union's Horizon 2020 research and innovation programme under grant agreement No 654109 for support of the ACTRIS network; and the Atmospheric Radiation Measurement (ARM) user facility, a U.S. Department of Energy (DOE) office of science user facility managed by the Biological and Environmental Research Program.

Author Contributions

Conceptualization: YZ, JM
Methodology: YZ, LWH, RM, DJP, VN, JM
Investigation: YZ, LWH, JM
Writing—original draft: YZ, JM
Writing—review & editing: YZ, LWH, RM, DJP, VN, JL, JM

Data availability

The IMPROVE filter OA and sulfate data is available at http://views.cira.colostate.edu/iwdw/. The ACTRIS ACSM OA data is available at https://actris.nilu.no/. The ARM ACSM OA data is available at https://www.arm.gov/data/. The EPA's AQS data is available at https://aqs.epa.gov. Model outputs are available at https://doi.org/10.6084/m9.figshare.21493986.v1.

Competing interests

The authors declare no competing interests.

1 References:

2 Blanchard, C. L., Hidy, G. M., Shaw, S., Baumann, K., and Edgerton, E. S.: Effects of emission
3 reductions on organic aerosol in the southeastern United States, Atmos. Chem. Phys., 16, 215–
4 238, https://doi.org/10.5194/acp-16-215-2016, 2016.

5 Boyd, C. M., Nah, T., Xu, L., Berkemeier, T., and Ng, N. L.: Secondary Organic Aerosol (SOA)
6 from Nitrate Radical Oxidation of Monoterpenes: Effects of Temperature, Dilution, and
7 Humidity on Aerosol Formation, Mixing, and Evaporation, Environmental Science &
8 Technology, 51, 7831–7841, https://doi.org/10.1021/acs.est.7b01460, 2017.

9 Carlton, A. G., Pinder, R. W., Bhave, P. V., and Pouliot, G. A.: To What Extent Can Biogenic
10 SOA be Controlled?, Environmental Science & Technology, 44, 3376–3380,
11 https://doi.org/10.1021/es903506b, 2010.

12 Carslaw, K. S., Lee, L. A., Reddington, C. L., Pringle, K. J., Rap, A., Forster, P. M., Mann, G.
13 W., Spracklen, D. V., Woodhouse, M. T., Regayre, L. A., and Pierce, J. R.: Large contribution of
14 natural aerosols to uncertainty in indirect forcing, Nature, 503, 67–71,
15 https://doi.org/10.1038/nature12674, 2013.

16 Chen, C., Zhang, Z., Wei, L., Qiu, Y., Xu, W., Song, S., Sun, J., Li, Z., Chen, Y., Ma, N., Xu,
17 W., Pan, X., Fu, P., and Sun, Y.: The importance of hydroxymethanesulfonate (HMS) in winter
18 haze episodes in North China Plain, Environmental Research, 211, 113093,
19 https://doi.org/10.1016/j.envres.2022.113093, 2022.

20 Crenn, V., Sciare, J., Croteau, P. L., Verlhac, S., Fröhlich, R., Belis, C. A., Aas, W., Äijälä, M.,
21 Alastuey, A., Artiñano, B., Baisnée, D., Bonnaire, N., Bressi, M., Canagaratna, M., Canonaco,
22 F., Carbone, C., Cavalli, F., Coz, E., Cubison, M. J., Esser-Gietl, J. K., Green, D. C., Gros, V.,
23 Heikkinen, L., Herrmann, H., Lunder, C., Minguillón, M. C., Močnik, G., O'Dowd, C. D.,
24 Ovadnevaite, J., Petit, J.-E., Petralia, E., Poulain, L., Priestman, M., Riffault, V., Ripoll, A.,
25 Sarda-Estève, R., Slowik, J. G., Setyan, A., Wiedensohler, A., Baltensperger, U., Prévôt, A. S.
26 H., Jayne, J. T., and Favez, O.: ACTRIS ACSM intercomparison – Part 1: Reproducibility of
27 concentration and fragment results from 13 individual Quadrupole Aerosol Chemical Speciation
28 Monitors (Q-ACSM) and consistency with co-located instruments, Atmospheric Measurement
29 Techniques, 8, 5063–5087, https://doi.org/10.5194/amt-8-5063-2015, 2015.

30 Donahue, N. M., Robinson, A. L., Stanier, C. O., and Pandis, S. N.: Coupled Partitioning,
31 Dilution, and Chemical Aging of Semivolatile Organics, Environmental Science & Technology,
32 40, 2635–2643, https://doi.org/10.1021/es052297c, 2006.

33 Donahue, N. M., Henry, K. M., Mentel, T. F., Kiendler-Scharr, A., Spindler, C., Bohn, B.,
34 Brauers, T., Dorn, H. P., Fuchs, H., Tillmann, R., Wahner, A., Saathoff, H., Naumann, K.-H.,
35 Möhler, O., Leisner, T., Müller, L., Reinnig, M.-C., Hoffmann, T., Salo, K., Hallquist, M.,
36 Frosch, M., Bilde, M., Tritscher, T., Barmet, P., Praplan, A. P., DeCarlo, P. F., Dommen, J.,
37 Prévôt, A. S. H., and Baltensperger, U.: Aging of biogenic secondary organic aerosol via gas-
38 phase OH radical reactions, Proceedings of the National Academy of Sciences, 109, 13503–
39 13508, https://doi.org/10.1073/pnas.1115186109, 2012.

1 Edgerton, E. S., Hartsell, B. E., Saylor, R. D., Jansen, J. J., Hansen, D. A., and Hidy, G. M.: The
2 Southeastern Aerosol Research and Characterization Study: Part II. Filter-Based Measurements
3 of Fine and Coarse Particulate Matter Mass and Composition, Journal of the Air & Waste
4 Management Association, 55, 1527–1542, https://doi.org/10.1080/10473289.2005.10464744,
5 2005.

6 Guenther, A. B., Jiang, X., Heald, C. L., Sakulyanontvittaya, T., Duhl, T., Emmons, L. K., and
7 Wang, X.: The Model of Emissions of Gases and Aerosols from Nature version 2.1
8 (MEGAN2.1): an extended and updated framework for modeling biogenic emissions, Geosci.
9 Model Dev., 5, 1471–1492, https://doi.org/10.5194/gmd-5-1471-2012, 2012.

10 Heald, C. L. and Geddes, J. A.: The impact of historical land use change from 1850 to 2000 on
11 secondary particulate matter and ozone, Atmospheric Chemistry and Physics, 16, 14997–15010,
12 https://doi.org/10.5194/acp-16-14997-2016, 2016.

13 Heald, C. L. and Spracklen, D. V.: Land Use Change Impacts on Air Quality and Climate,
14 Chemical Reviews, 115, 4476–4496, https://doi.org/10.1021/cr500446g, 2015.

15 Henze, D. K. and Seinfeld, J. H.: Global secondary organic aerosol from isoprene oxidation,
16 Geophysical Research Letters, 33, L09812, https://doi.org/10.1029/2006gl025976, 2006.

17 Horowitz, L. W., Naik, V., Paulot, F., Ginoux, P. A., Dunne, J. P., Mao, J., Schnell, J., Chen, X.,
18 He, J., John, J. G., Lin, M., Lin, P., Malyshev, S., Paynter, D., Shevliakova, E., and Zhao, M.:
19 The GFDL Global Atmospheric Chemistry-Climate Model AM4.1: Model Description and
20 Simulation Characteristics, Journal of Advances in Modeling Earth Systems, 12,
21 e2019MS002032, https://doi.org/10.1029/2019MS002032, 2020.

22 Hoyle, C. R., Myhre, G., Berntsen, T. K., and Isaksen, I. S. A.: Anthropogenic influence on SOA
23 and the resulting radiative forcing, Atmospheric Chemistry and Physics, 9, 2715–2728,
24 https://doi.org/10.5194/acp-9-2715-2009, 2009.

25 Hoyle, C. R., Boy, M., Donahue, N. M., Fry, J. L., Glasius, M., Guenther, A., Hallar, A. G., Huff
26 Hartz, K., Petters, M. D., Petäjä, T., Rosenoern, T., and Sullivan, A. P.: A review of the
27 anthropogenic influence on biogenic secondary organic aerosol, Atmospheric Chemistry and
28 Physics, 11, 321–343, https://doi.org/10.5194/acp-11-321-2011, 2011.

29 Isaacman-VanWertz, G., Massoli, P., O'Brien, R., Lim, C., Franklin, J. P., Moss, J. A., Hunter, J.
30 F., Nowak, J. B., Canagaratna, M. R., Misztal, P. K., Arata, C., Roscioli, J. R., Herndon, S. T.,
31 Onasch, T. B., Lambe, A. T., Jayne, J. T., Su, L., Knopf, D. A., Goldstein, A. H., Worsnop, D.
32 R., and Kroll, J. H.: Chemical evolution of atmospheric organic carbon over multiple generations
33 of oxidation, Nature Chem, 10, 462–468, https://doi.org/10.1038/s41557-018-0002-2, 2018.

34 Jiang, J., Aksoyoglu, S., Ciarelli, G., Oikonomakis, E., El-Haddad, I., Canonaco, F., O'Dowd,
35 C., Ovadnevaite, J., Minguillón, M. C., Baltensperger, U., and Prévôt, A. S. H.: Effects of two
36 different biogenic emission models on modelled ozone and aerosol concentrations in Europe,
37 Atmospheric Chemistry and Physics, 19, 3747–3768, https://doi.org/10.5194/acp-19-3747-2019,
38 2019.

1   Kroll, J. H. and Seinfeld, J. H.: Chemistry of secondary organic aerosol: Formation and evolution
2   of low-volatility organics in the atmosphere, Atmospheric Environment, 42, 3593–3624,
3   https://doi.org/10.1016/j.atmosenv.2008.01.003, 2008.

4   Kroll, J. H., Ng, N. L., Murphy, S. M., Varutbangkul, V., Flagan, R. C., and Seinfeld, J. H.:
5   Chamber studies of secondary organic aerosol growth by reactive uptake of simple carbonyl
6   compounds, Journal of Geophysical Research: Atmospheres, 110, n/a-n/a,
7   https://doi.org/10.1029/2005JD006004, 2005.

8   Li, J., Mao, J., Min, K.-E., Washenfelder, R. A., Brown, S. S., Kaiser, J., Keutsch, F. N.,
9   Volkamer, R., Wolfe, G. M., Hanisco, T. F., Pollack, I. B., Ryerson, T. B., Graus, M., Gilman, J.
10 B., Lerner, B. M., Warneke, C., de Gouw, J. A., Middlebrook, A. M., Liao, J., Welti, A.,
11 Henderson, B. H., McNeill, V. F., Hall, S. R., Ullmann, K., Donner, L. J., Paulot, F., and
12 Horowitz, L. W.: Observational constraints on glyoxal production from isoprene oxidation and
13 its contribution to organic aerosol over the Southeast United States, Journal of Geophysical
14 Research: Atmospheres, 121, 9849–9861, https://doi.org/10.1002/2016JD025331, 2016.

15 Li, J., Mao, J., Fiore, A. M., Cohen, R. C., Crounse, J. D., Teng, A. P., Wennberg, P. O., Lee, B.
16 H., Lopez-Hilfiker, F. D., Thornton, J. A., Peischl, J., Pollack, I. B., Ryerson, T. B., Veres, P.,
17 Roberts, J. M., Neuman, J. A., Nowak, J. B., Wolfe, G. M., Hanisco, T. F., Fried, A., Singh, H.
18 B., Dibb, J., Paulot, F., and Horowitz, L. W.: Decadal changes in summertime reactive oxidized
19 nitrogen and surface ozone over the Southeast United States, Atmospheric Chemistry and
20 Physics, 18, 2341–2361, https://doi.org/10.5194/acp-18-2341-2018, 2018.

21 Lin, G., Sillman, S., Penner, J. E., and Ito, A.: Global modeling of SOA: the use of different
22 mechanisms for aqueous-phase formation, Atmos. Chem. Phys., 14, 5451–5475,
23 https://doi.org/10.5194/acp-14-5451-2014, 2014a.

24 Lin, G., Penner, J. E., Flanner, M. G., Sillman, S., Xu, L., and Zhou, C.: Radiative forcing of
25 organic aerosol in the atmosphere and on snow: Effects of SOA and brown carbon, Journal of
26 Geophysical Research: Atmospheres, 119, 7453–7476, https://doi.org/10.1002/2013JD021186,
27 2014b.

28 Liu, Y., Dong, X., Wang, M., Emmons, L. K., Liu, Y., Liang, Y., Li, X., and Shrivastava, M.:
29 Analysis of secondary organic aerosol simulation bias in the Community Earth System Model
30 (CESM2.1), Atmospheric Chemistry and Physics, 21, 8003–8021, https://doi.org/10.5194/acp-
31 21-8003-2021, 2021.

32 Mao, J., Horowitz, L. W., Naik, V., Fan, S., Liu, J., and Fiore, A. M.: Sensitivity of tropospheric
33 oxidants to biomass burning emissions: implications for radiative forcing, Geophysical Research
34 Letters, 40, 1241–1246, https://doi.org/10.1002/grl.50210, 2013.

35 Mao, J., Carlton, A., Cohen, R. C., Brune, W. H., Brown, S. S., Wolfe, G. M., Jimenez, J. L.,
36 Pye, H. O. T., Lee Ng, N., Xu, L., McNeill, V. F., Tsigaridis, K., McDonald, B. C., Warneke, C.,
37 Guenther, A., Alvarado, M. J., Gouw, J. de, Mickley, L. J., Leibensperger, E. M., Mathur, R.,
38 Nolte, C. G., Portmann, R. W., Unger, N., Tosca, M., and Horowitz, L. W.: Southeast
39 Atmosphere Studies: learning from model-observation syntheses, Atmospheric Chemistry and
40 Physics, 18, 2615–2651, https://doi.org/10.5194/acp-18-2615-2018, 2018.

1 Marais, E. A., Jacob, D. J., Jimenez, J. L., Campuzano-Jost, P., Day, D. A., Hu, W., Krechmer,
2 J., Zhu, L., Kim, P. S., Miller, C. C., Fisher, J. A., Travis, K., Yu, K., Hanisco, T. F., Wolfe, G.
3 M., Arkinson, H. L., Pye, H. O. T., Froyd, K. D., Liao, J., and McNeill, V. F.: Aqueous-phase
4 mechanism for secondary organic aerosol formation from isoprene: application to the southeast
5 United States and co-benefit of SO2 emission controls, Atmos. Chem. Phys., 16, 1603–1618,
6 https://doi.org/10.5194/acp-16-1603-2016, 2016.

7 Marais, E. A., Jacob, D. J., Turner, J. R., and Mickley, L. J.: Evidence of 1991–2013 decrease of
8 biogenic secondary organic aerosol in response to SO 2 emission controls, Environmental
9 Research Letters, 12, 054018, 2017.

10 Ng, N. L., Brown, S. S., Archibald, A. T., Atlas, E., Cohen, R. C., Crowley, J. N., Day, D. A.,
11 Donahue, N. M., Fry, J. L., Fuchs, H., Griffin, R. J., Guzman, M. I., Herrmann, H., Hodzic, A.,
12 Iinuma, Y., Jimenez, J. L., Kiendler-Scharr, A., Lee, B. H., Luecken, D. J., Mao, J., McLaren, R.,
13 Mutzel, A., Osthoff, H. D., Ouyang, B., Picquet-Varrault, B., Platt, U., Pye, H. O. T., Rudich, Y.,
14 Schwantes, R. H., Shiraiwa, M., Stutz, J., Thornton, J. A., Tilgner, A., Williams, B. J., and
15 Zaveri, R. A.: Nitrate radicals and biogenic volatile organic compounds: oxidation, mechanisms,
16 and organic aerosol, Atmos. Chem. Phys., 17, 2103–2162, https://doi.org/10.5194/acp-17-2103-
17 2017, 2017.

18 Pai, S. J., Heald, C. L., Pierce, J. R., Farina, S. C., Marais, E. A., Jimenez, J. L., Campuzano-
19 Jost, P., Nault, B. A., Middlebrook, A. M., Coe, H., Shilling, J. E., Bahreini, R., Dingle, J. H.,
20 and Vu, K.: An evaluation of global organic aerosol schemes using airborne observations,
21 Atmospheric Chemistry and Physics, 20, 2637–2665, https://doi.org/10.5194/acp-20-2637-2020,
22 2020.

23 Pai, S. J., Carter, T. S., Heald, C. L., and Kroll, J. H.: Updated World Health Organization Air
24 Quality Guidelines Highlight the Importance of Non-anthropogenic PM2.5, Environ. Sci.
25 Technol. Lett., 9, 501–506, https://doi.org/10.1021/acs.estlett.2c00203, 2022.

26 Pandis, S. N., Harley, R. A., Cass, G. R., and Seinfeld, J. H.: Secondary organic aerosol
27 formation and transport, Atmospheric Environment. Part A. General Topics, 26, 2269–2282,
28 https://doi.org/10.1016/0960-1686(92)90358-R, 1992.

29 Paulot, F., Crounse, J. D., Kjaergaard, H. G., Kurten, A., St Clair, J. M., Seinfeld, J. H., and
30 Wennberg, P. O.: Unexpected Epoxide Formation in the Gas-Phase Photooxidation of Isoprene,
31 Science, 325, 730–733, https://doi.org/10.1126/science.1172910, 2009.

32 Philip, S., Martin, R. V., Pierce, J. R., Jimenez, J. L., Zhang, Q., Canagaratna, M. R., Spracklen,
33 D. V., Nowlan, C. R., Lamsal, L. N., Cooper, M. J., and Krotkov, N. A.: Spatially and seasonally
34 resolved estimate of the ratio of organic mass to organic carbon, Atmospheric Environment, 87,
35 34–40, https://doi.org/10.1016/j.atmosenv.2013.11.065, 2014.

36 Presto, A. A., Huff Hartz, K. E., and Donahue, N. M.: Secondary Organic Aerosol Production
37 from Terpene Ozonolysis. 2. Effect of NOx Concentration, Environmental Science &
38 Technology, 39, 7046–7054, https://doi.org/10.1021/es050400s, 2005.

1   Pye, H. O. T., Chan, A. W. H., Barkley, M. P., and Seinfeld, J. H.: Global modeling of organic
2   aerosol: the importance of reactive nitrogen (NOx and NO3), Atmospheric Chemistry and
3   Physics, 10, 11261–11276, https://doi.org/10.5194/acp-10-11261-2010, 2010.

4   Pye, H. O. T., Pinder, R. W., Piletic, I. R., Xie, Y., Capps, S. L., Lin, Y.-H., Surratt, J. D., Zhang,
5   Z., Gold, A., Luecken, D. J., Hutzell, W. T., Jaoui, M., Offenberg, J. H., Kleindienst, T. E.,
6   Lewandowski, M., and Edney, E. O.: Epoxide Pathways Improve Model Predictions of Isoprene
7   Markers and Reveal Key Role of Acidity in Aerosol Formation, Environ. Sci. Technol., 47,
8   11056–11064, https://doi.org/10.1021/es402106h, 2013.

9   Pye, H. O. T., D'Ambro, E. L., Lee, B. H., Schobesberger, S., Takeuchi, M., Zhao, Y., Lopez-
10 Hilfiker, F., Liu, J., Shilling, J. E., Xing, J., Mathur, R., Middlebrook, A. M., Liao, J., Welti, A.,
11 Graus, M., Warneke, C., de Gouw, J. A., Holloway, J. S., Ryerson, T. B., Pollack, I. B., and
12 Thornton, J. A.: Anthropogenic enhancements to production of highly oxygenated molecules
13 from autoxidation, Proc Natl Acad Sci USA, 116, 6641–6646,
14 https://doi.org/10.1073/pnas.1810774116, 2019.

15 Pye, H. O. T., Ward-Caviness, C. K., Murphy, B. N., Appel, K. W., and Seltzer, K. M.:
16 Secondary organic aerosol association with cardiorespiratory disease mortality in the United
17 States, Nat Commun, 12, 7215, https://doi.org/10.1038/s41467-021-27484-1, 2021.

18 Ridley, D. A., Heald, C. L., Ridley, K. J., and Kroll, J. H.: Causes and consequences of
19 decreasing atmospheric organic aerosol in the United States, Proc Natl Acad Sci USA, 115, 290–
20 295, https://doi.org/10.1073/pnas.1700387115, 2018.

21 Robinson, A. L., Donahue, N. M., Shrivastava, M. K., Weitkamp, E. A., Sage, A. M., Grieshop,
22 A. P., Lane, T. E., Pierce, J. R., and Pandis, S. N.: Rethinking Organic Aerosols: Semivolatile
23 Emissions and Photochemical Aging, Science, 315, 1259–1262,
24 https://doi.org/10.1126/science.1133061, 2007.

25 Rollins, A. W., Browne, E. C., Min, K.-E., Pusede, S. E., Wooldridge, P. J., Gentner, D. R.,
26 Goldstein, A. H., Liu, S., Day, D. A., Russell, L. M., and Cohen, R. C.: Evidence for NOx
27 Control over Nighttime SOA Formation, Science, 337, 1210–1212,
28 https://doi.org/10.1126/science.1221520, 2012.

29 Scott, C. E., Monks, S. A., Spracklen, D. V., Arnold, S. R., Forster, P. M., Rap, A., Carslaw, K.
30 S., Chipperfield, M. P., Reddington, C. L. S., and Wilson, C.: Impact on short-lived climate
31 forcers (SLCFs) from a realistic land-use change scenario via changes in biogenic emissions,
32 Faraday Discuss., 200, 101–120, https://doi.org/10.1039/C7FD00028F, 2017.

33 Shrivastava, M., Cappa, C. D., Fan, J., Goldstein, A. H., Guenther, A. B., Jimenez, J. L., Kuang,
34 C., Laskin, A., Martin, S. T., Ng, N. L., Petaja, T., Pierce, J. R., Rasch, P. J., Roldin, P., Seinfeld,
35 J. H., Shilling, J., Smith, J. N., Thornton, J. A., Volkamer, R., Wang, J., Worsnop, D. R., Zaveri,
36 R. A., Zelenyuk, A., and Zhang, Q.: Recent advances in understanding secondary organic
37 aerosol: Implications for global climate forcing, Reviews of Geophysics, 55, 509–559,
38 https://doi.org/10.1002/2016RG000540, 2017.

1   Simon, H., Reff, A., Wells, B., Xing, J., and Frank, N.: Ozone Trends Across the United States
2   over a Period of Decreasing NOx and VOC Emissions, Environ. Sci. Technol., 49, 186–195,
3   https://doi.org/10.1021/es504514z, 2015.

4   Solomon, P. A., Crumpler, D., Flanagan, J. B., Jayanty, R. K. M., Rickman, E. E., and McDade,
5   C. E.: U.S. National PM2.5 Chemical Speciation Monitoring Networks—CSN and IMPROVE:
6   Description of networks, Journal of the Air & Waste Management Association, 64, 1410–1438,
7   https://doi.org/10.1080/10962247.2014.956904, 2014.

8   Spracklen, D. V., Jimenez, J. L., Carslaw, K. S., Worsnop, D. R., Evans, M. J., Mann, G. W.,
9   Zhang, Q., Canagaratna, M. R., Allan, J., Coe, H., McFiggans, G., Rap, A., and Forster, P.:
10 Aerosol mass spectrometer constraint on the global secondary organic aerosol budget, Atmos.
11 Chem. Phys., 11, 12109–12136, https://doi.org/10.5194/acp-11-12109-2011, 2011.

12 Tsigaridis, K., Daskalakis, N., Kanakidou, M., Adams, P. J., Artaxo, P., Bahadur, R., Balkanski,
13 Y., Bauer, S. E., Bellouin, N., Benedetti, A., Bergman, T., Berntsen, T. K., Beukes, J. P., Bian,
14 H., Carslaw, K. S., Chin, M., Curci, G., Diehl, T., Easter, R. C., Ghan, S. J., Gong, S. L., Hodzic,
15 A., Hoyle, C. R., Iversen, T., Jathar, S., Jimenez, J. L., Kaiser, J. W., Kirkevåg, A., Koch, D.,
16 Kokkola, H., Lee, Y. H., Lin, G., Liu, X., Luo, G., Ma, X., Mann, G. W., Mihalopoulos, N.,
17 Morcrette, J. J., Müller, J. F., Myhre, G., Myriokefalitakis, S., Ng, N. L., O'Donnell, D., Penner,
18 J. E., Pozzoli, L., Pringle, K. J., Russell, L. M., Schulz, M., Sciare, J., Seland, Ø., Shindell, D. T.,
19 Sillman, S., Skeie, R. B., Spracklen, D., Stavrakou, T., Steenrod, S. D., Takemura, T., Tiitta, P.,
20 Tilmes, S., Tost, H., van Noije, T., van Zyl, P. G., von Salzen, K., Yu, F., Wang, Z., Wang, Z.,
21 Zaveri, R. A., Zhang, H., Zhang, K., Zhang, Q., and Zhang, X.: The AeroCom evaluation and
22 intercomparison of organic aerosol in global models, Atmos. Chem. Phys., 14, 10845–10895,
23 https://doi.org/10.5194/acp-14-10845-2014, 2014.

24 Uin, J., Aiken, A. C., Dubey, M. K., Kuang, C., Pekour, M., Salwen, C., Sedlacek, A. J., Senum,
25 G., Smith, S., Wang, J., Watson, T. B., and Springston, S. R.: Atmospheric Radiation
26 Measurement (ARM) Aerosol Observing Systems (AOS) for Surface-Based In Situ Atmospheric
27 Aerosol and Trace Gas Measurements, Journal of Atmospheric and Oceanic Technology, 36,
28 2429–2447, https://doi.org/10.1175/JTECH-D-19-0077.1, 2019.

29 Unger, N.: Human land-use-driven reduction of forest volatiles cools global climate, Nature
30 Clim Change, 4, 907–910, https://doi.org/10.1038/nclimate2347, 2014.

31 Wells, B., Dolwick, P., Eder, B., Evangelista, M., Foley, K., Mannshardt, E., Misenis, C., and
32 Weishampel, A.: Improved estimation of trends in U.S. ozone concentrations adjusted for
33 interannual variability in meteorological conditions, Atmospheric Environment, 248, 118234,
34 https://doi.org/10.1016/j.atmosenv.2021.118234, 2021.

35 Whaley, C. H., Mahmood, R., von Salzen, K., Winter, B., Eckhardt, S., Arnold, S., Beagley, S.,
36 Becagli, S., Chien, R.-Y., Christensen, J., Damani, S. M., Dong, X., Eleftheriadis, K.,
37 Evangeliou, N., Faluvegi, G., Flanner, M., Fu, J. S., Gauss, M., Giardi, F., Gong, W., Hjorth, J.
38 L., Huang, L., Im, U., Kanaya, Y., Krishnan, S., Klimont, Z., Kühn, T., Langner, J., Law, K. S.,
39 Marelle, L., Massling, A., Olivié, D., Onishi, T., Oshima, N., Peng, Y., Plummer, D. A.,
40 Popovicheva, O., Pozzoli, L., Raut, J.-C., Sand, M., Saunders, L. N., Schmale, J., Sharma, S.,

1 Skeie, R. B., Skov, H., Taketani, F., Thomas, M. A., Traversi, R., Tsigaridis, K., Tsyro, S.,
2 Turnock, S., Vitale, V., Walker, K. A., Wang, M., Watson-Parris, D., and Weiss-Gibbons, T.:
3 Model evaluation of short-lived climate forcers for the Arctic Monitoring and Assessment
4 Programme: a multi-species, multi-model study, Atmospheric Chemistry and Physics, 22, 5775–
5 5828, https://doi.org/10.5194/acp-22-5775-2022, 2022.

6 Xu, L., Pye, H. O. T., He, J., Chen, Y., Murphy, B. N., and Ng, N. L.: Experimental and model
7 estimates of the contributions from biogenic monoterpenes and sesquiterpenes to secondary
8 organic aerosol in the southeastern United States, Atmos. Chem. Phys., 18, 12613–12637,
9 https://doi.org/10.5194/acp-18-12613-2018, 2018.

10 Zhang, H., Yee, L. D., Lee, B. H., Curtis, M. P., Worton, D. R., Isaacman-VanWertz, G.,
11 Offenberg, J. H., Lewandowski, M., Kleindienst, T. E., Beaver, M. R., Holder, A. L., Lonneman,
12 W. A., Docherty, K. S., Jaoui, M., Pye, H. O. T., Hu, W., Day, D. A., Campuzano-Jost, P.,
13 Jimenez, J. L., Guo, H., Weber, R. J., de Gouw, J., Koss, A. R., Edgerton, E. S., Brune, W.,
14 Mohr, C., Lopez-Hilfiker, F. D., Lutz, A., Kreisberg, N. M., Spielman, S. R., Hering, S. V.,
15 Wilson, K. R., Thornton, J. A., and Goldstein, A. H.: Monoterpenes are the largest source of
16 summertime organic aerosol in the southeastern United States, Proceedings of the National
17 Academy of Sciences, 115, 2038–2043, https://doi.org/10.1073/pnas.1717513115, 2018a.

18 Zhang, Y., Chen, Y., Lambe, A. T., Olson, N. E., Lei, Z., Craig, R. L., Zhang, Z., Gold, A.,
19 Onasch, T. B., Jayne, J. T., Worsnop, D. R., Gaston, C. J., Thornton, J. A., Vizuete, W., Ault, A.
20 P., and Surratt, J. D.: Effect of the Aerosol-Phase State on Secondary Organic Aerosol Formation
21 from the Reactive Uptake of Isoprene-Derived Epoxydiols (IEPOX), Environmental Science &
22 Technology Letters, 5, 167–174, https://doi.org/10.1021/acs.estlett.8b00044, 2018b.

23 Zheng, Y., Unger, N., Hodzic, A., Emmons, L., Knote, C., Tilmes, S., Lamarque, J. F., and Yu,
24 P.: Limited effect of anthropogenic nitrogen oxides on secondary organic aerosol formation,
25 Atmos. Chem. Phys., 15, 13487–13506, https://doi.org/10.5194/acp-15-13487-2015, 2015.

26 Zheng, Y., Thornton, J. A., Ng, N. L., Cao, H., Henze, D. K., McDuffie, E. E., Hu, W., Jimenez,
27 J. L., Marais, E. A., Edgerton, E., and Mao, J.: Long-term observational constraints of organic
28 aerosol dependence on inorganic species in the southeast US, Atmospheric Chemistry and
29 Physics, 20, 13091–13107, https://doi.org/10.5194/acp-20-13091-2020, 2020.

30 Zhu, J., Penner, J. E., Yu, F., Sillman, S., Andreae, M. O., and Coe, H.: Decrease in radiative
31 forcing by organic aerosol nucleation, climate, and land use change, Nat Commun, 10, 423,
32 https://doi.org/10.1038/s41467-019-08407-7, 2019.

33

34

Table 1. Comparison of the SOA schemes used in this study. Further details and discussions are included in Methods.

Scheme	ASOA	ISOA	TSOA					
			10% yields from monoterpene emissions					
			4-bin VBS[2]	α for C* (C* in µg/m³)				Yield at 10 µg/m³
				C*=0.1	C*=1	C*=10	C*=100	
Simple	C_4H_{10}+OH	10% yields from isoprene emissions						
CMPX	Same as Simple	Heterogeneous uptake of IEPOX (γ=0.001) and glyoxal (γ=0.001)[1]	MTP+OH/O_3; NO (high-NO$_x$ pathway)	0.04	0.0095	0.09	0.015	0.09
			MTP+OH/O_3; HO_2 (low-NO$_x$ pathway)	0.08	0.019	0.18	0.03	0.19
			MTP+NO_3	0	0	0.321	1.083	0.26
CMPX_ag[3]	Same as Simple	Same as CMPX	Same as CMPX, with aging k_{OH} = 4×10⁻¹¹ cm³ molec⁻¹ s⁻¹					

[1] γ represents uptake coefficients of IEPOX or glyoxal onto aqueous sulfate aerosol.

[2] In the 4-bin VBS, monoterpene (MTP) is oxidized by OH, O_3 or NO_3 to generate 4 semivolatile surrogate products, which can reversibly partition into pre-existing organic aerosol. C* represents saturation concentration of each semivolatile product and determines the partitioning of these products between gas and aerosol phase. The mass-based stoichiometric yield coefficients, α, for each parent hydrocarbon/oxidant system are fit with a VBS using C* of 0.1, 1, 10, and 100 µg/m³ (Pye et al. 2010).

[3] In the aging scheme, at every time step, each semivolatile product except for the lowest volatility bin (C*=0.1 µg m⁻³) is assumed to be further oxidized by OH with a rate constant of k_{OH} = 4×10⁻¹¹ cm³ molec⁻¹ s⁻¹, which reduces its volatility by an order of magnitude.

Table 2. Annual mean budget of POA and SOA in all simulations. Results are averaged over 1872-1888 for pre-industrial and 2000-2016 for present-day simulations. SOA includes ASOA (anthropogenic SOA), ISOA (isoprene-SOA), and TSOA (monoterpene-SOA).

Simulation	Variable	PI					PD				
		Burden (Tg)	Production (Tg/yr)	Wet Deposition (Tg/yr)	Dry Deposition (Tg/yr)	Lifetime (day)	Burden (Tg)	Production (Tg/yr)	Wet Deposition (Tg/yr)	Dry Deposition (Tg/yr)	Lifetime (day)
All[1]	POA	0.58	47.0	32.4	14.6	4.5	1.00	68.1	48.9	19.2	5.4
Simple	ASOA	0.003	0.2	-	-	-	0.06	3.3	-	-	-
	ISOA	0.83	80.4	-	-	-	0.78	65.0	-	-	-
	TSOA	0.15	15.6	-	-	-	0.15	13.4	-	-	-
	Total SOA	0.98	96.2	79.3	16.9	3.7	0.99	81.7	68.0	13.7	4.4
CMPX	ASOA	0.003	0.2	-	-	-	0.06	3.3	-	-	-
	ISOA	0.11	10.7	-	-	-	0.26	22.2	-	-	-
	TSOA	0.16	15.5	-	-	-	0.17	14.4	-	-	-
	Total SOA	0.27	26.4	22.3	4.1	3.7	0.50	39.9	33.6	6.3	4.6
CMPX_ag	ASOA	0.003	0.2	-	-	-	0.06	3.3	-	-	-
	ISOA	0.11	10.8	-	-	-	0.27	22.0	-	-	-
	TSOA	0.63	40.1	-	-	-	0.72	44.0	-	-	-
	Total SOA	0.74	51.1	43.4	7.7	5.3	1.05	69.3	58.9	10.4	5.5

[1]For POA budget, the differences between different schemes are negligible.
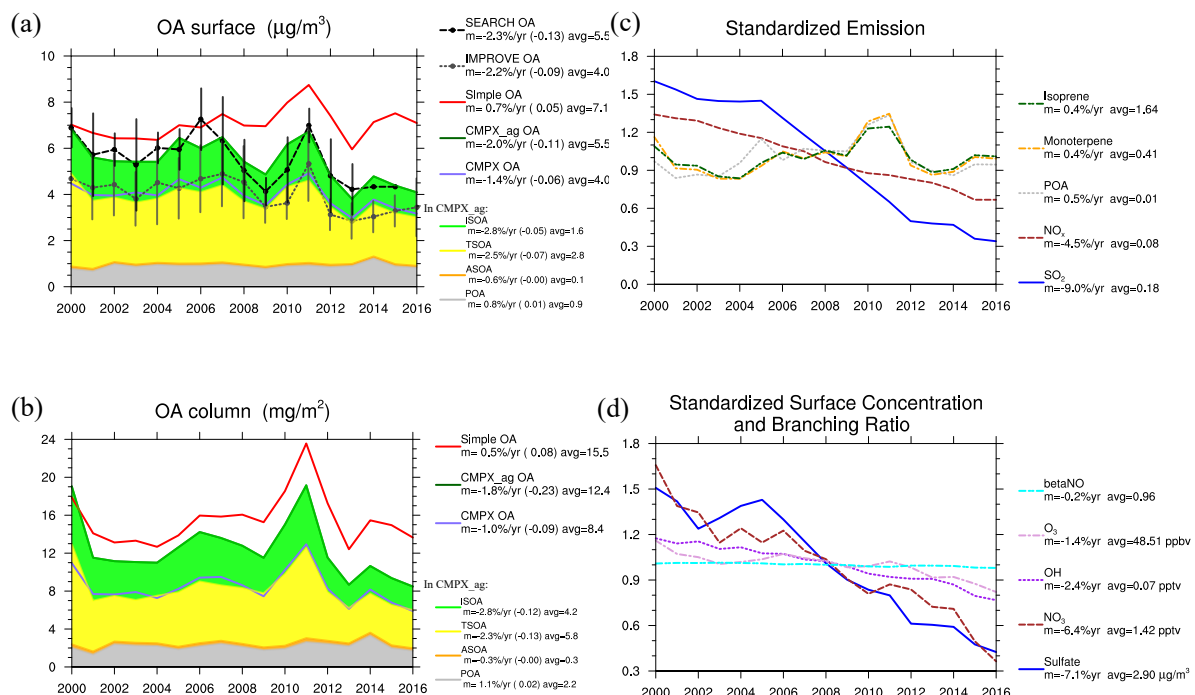
Figure 1. Summertime (June-July-August) values averaged in the southeast US in 2000-2016. **(a)** Surface concentrations of OA from the two measurement networks, IMPROVE and SEARCH, and the Simple, CMPX and CMPX_ag simulations. **(b)** Column concentrations of OA. In (a) and (b), color shades represent OA components from the CMPX_ag scheme. **(c)** Standardized emissions of isoprene, monoterpenes, POA, NO_x and SO_2. **(d)** Standardized surface concentrations of gases O_3, OH and NO_3, sulfate aerosol, and branching ratio. In (c) and (d), each variable has been divided by its 17-year average for standardization. In attached text, "m" represents 2000-2016 relative trend with units of %/year; numbers in parenthesis in (a) and (b) represent trends with units of $\mu g/m^3$/year or mg/m^2/year; "avg" represents the 17-year average with units of $\mu g/m^3$ in (a), mg/m^2 in (b), mg/m^2/hour in (c) and different units shown in (d).
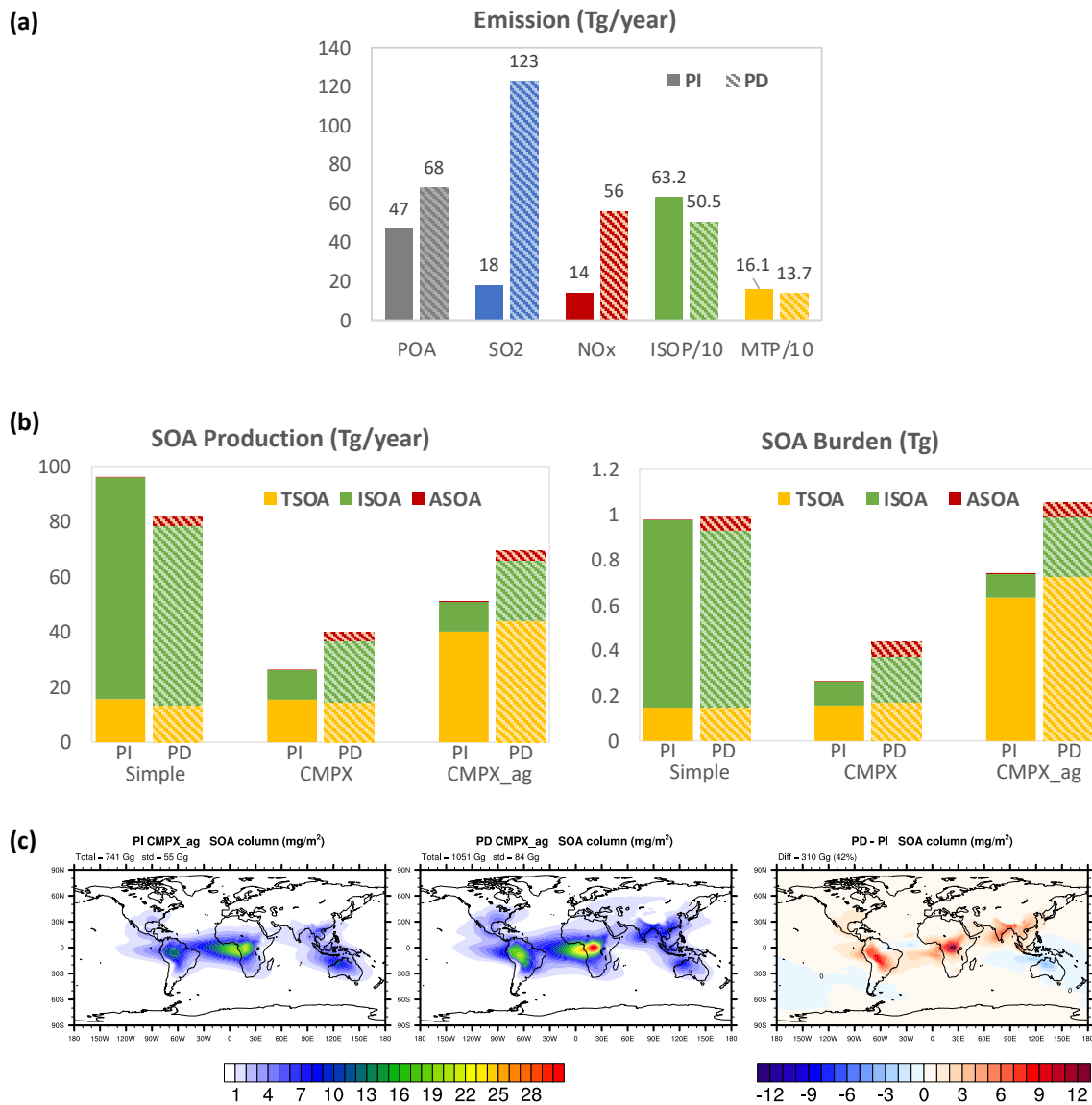
Figure 2. (a) Emissions (Tg/year) of POA, SO$_2$, NO$_x$, isoprene (ISOP) and monoterpenes (MTP). ISOP and MTP emissions have been divided by 10. **(b)** Simulated SOA global production (Tg/year) and burden (Tg). **(c)** Simulated SOA column concentration (mg/m^2) at PI and PD and their difference in the CMPX_ag scheme.
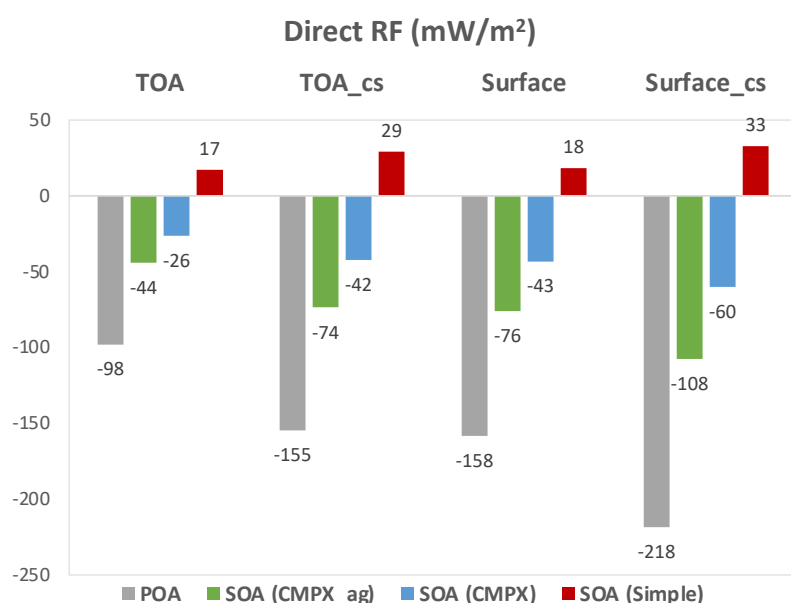
Figure 3. Direct radiative forcing (RF, mW/m²) of POA and SOA at top-of-atmosphere (TOA) all-sky, TOA clear-sky (TOA_cs), surface all-sky and surface clear-sky (Surface_cs) conditions. Negative RFs represent cooling effects.